

Rate-equation model of spin dynamics and polarized light emission for spin light-emitting diodes

Oliver Brandt,* Manfred Ramsteiner, Timur Flissikowski, Jens Herfort, and Holger T. Grahn
Paul-Drude-Institut für Festkörperelektronik, Hausvogteiplatz 5-7, 10117 Berlin, Germany
 (Received 3 September 2009; revised manuscript received 15 January 2010; published 2 March 2010)

We measure the circular polarization of the electroluminescence of $\text{Co}_2\text{FeSi}/(\text{Al,Ga})\text{As}/\text{GaAs}$ spin light-emitting diodes in magnetic fields up to 14 T. The observed polarization dependence varies greatly from sample to sample and often eludes an intuitive physical interpretation. We analyze our experimental data by a rate-equation model which explicitly takes into account the transport of carriers from the spin injector to the quantum well and their recombination therein. We show that our experimental data can be understood as an interplay of electron spin injection by the ferromagnetic overlayer and spin alignment in the layers the electrons are traversing before recombining in the quantum well. The main parameter controlling the electron spin polarization is identified to be the ratio of the transit time through these layers to the spin-scattering time in them.

DOI: [10.1103/PhysRevB.81.115302](https://doi.org/10.1103/PhysRevB.81.115302)

PACS number(s): 72.25.Hg, 72.25.Dc, 72.25.Mk, 72.25.Rb

I. INTRODUCTION

The generation of spin-polarized carriers in semiconductors is an essential prerequisite for spintronic applications, for which electrical spin injection from ferromagnetic metals has been proven to be a viable method.¹⁻⁵ For a quantitative evaluation of the spin-injection efficiency, spin light-emitting diodes (spin-LEDs) are commonly utilized. In the limit of negligible spin relaxation in the semiconductor structure, the spin-injection efficiency equals the polarization degree ρ_C of the electroluminescence (EL) emitted by the spin-LED containing a quantum well (QW) in the active region. In several studies, the spin and recombination dynamics within the embedded QW were taken into account via the experimentally determined exciton lifetime and spin-relaxation rates.⁴⁻⁷ However, what has been neglected in all previous studies of actual spin-LEDs is the separate transport of electrons and holes to the QW and the spin scattering of electrons on this way. This transport process has been presumed to be sufficiently fast to bypass all spin-scattering events.

Recently, we have investigated $\text{Co}_2\text{FeSi}/(\text{Al,Ga})\text{As}/\text{GaAs}$ spin-LEDs whose EL exhibits a circular polarization of up to 17%, and an experimentally confirmed injection efficiency of at least 50%. In the course of this work,⁸ we have also obtained firm evidence demonstrating that the above assumption of negligible spin scattering of electrons on their way to the active region is not generally valid. Co_2FeSi is (in its ordered $L2_1$ structure) a Heusler alloy, which is predicted to be a half-metal (i.e., providing electrons with one definitive spin direction only), and has the advantage to be closely lattice matched to GaAs allowing for the synthesis of high-quality epitaxial layers on $(\text{Al,Ga})\text{As}$.^{9,10} Indeed, in the meantime we have obtained devices exhibiting a circular EL polarization of up to 25%, which together with the previously determined values for the spin relaxation and exciton decay times in our structures⁸ amounts to an injection efficiency of 75% comparable to the state of the art in this field.^{2,4,11} Still, the injection efficiency is not close to the 100% expected when using a half-metallic injector, but just on par with more conventional approaches. Furthermore, the devices prove to be extremely sensitive to

subtle changes in preparation conditions and show a surprisingly wide variety in their electro-optical characteristics. Particularly, the dependence of ρ_C on the magnetic field B varies widely from sample to sample.

The key for the understanding of the complex behavior observed is the massive diffusion of Co and Fe into the topmost $(\text{Al,Ga})\text{As}$ layer as observed by secondary-ion mass spectrometry (SIMS), and as shown exemplary for two samples of relevance for the present paper in Fig. 1. Evidently, depending on the growth (or annealing) temperatures, this diffusion process may result in the substitutional incorporation of Co and Fe with a concentration exceeding one percent, thus converting the topmost $(\text{Al,Ga})\text{As}$ layer into a paramagnetic dilute magnetic semiconductor (DMS). Consequently, spin injection from the ferromagnetic Co_2FeSi layer may compete with ultrafast spin alignment in the $(\text{Al,Ga})\text{As}:(\text{Co,Fe})$ DMS.

Since diffusion is strictly thermally activated, the traditional remedy of diffusion-related issues is simply a reduction in the temperature used during the synthesis or processing of the structure under investigation. In the present case, we went as far as growing the Co_2FeSi layer without intentionally heating the substrate. Due to radiative heating from the Co, Fe, and Si high-temperature effusion cells (which are typically set to a temperature of 1465, 1200, and 1295 °C,

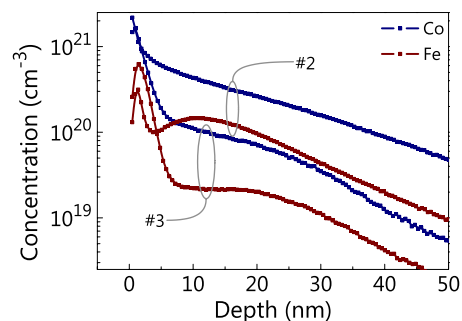


FIG. 1. (Color online) Fe and Co depth profiles as measured by SIMS for samples #2 and #3 in this paper. The Fe/Si₂ mass interference has been avoided by using an appropriate spectral resolution.

respectively), the minimum substrate temperature that can be obtained in this way is about 100 °C.

Lower substrate temperatures might be achieved with an active cooling of the substrate, but would actually be counterproductive. In fact, our previous investigations have shown that the desired L₂₁ ordering of the Co₂FeSi layer requires a growth temperature of at least 200 °C.^{9,10} At lower temperatures, we observe a B2 ordering, naturally excluding any half metallicity of the material. Attempts to circumvent the diffusion of Co and Fe into (Al,Ga)As thus require a radically different strategy possibly involving diffusion barriers and postgrowth annealing, both of which are *not* subject of the present work.

In this paper, we analyze the complex polarization response observed experimentally for Co₂FeSi/(Al,Ga)As/GaAs spin-LEDs using a rate-equation model which includes the transport of carriers, particularly electrons, to the QW and their recombination therein, thus taking into account both injection and alignment of electron spins in the layers the electrons are traversing prior to recombination. This model allows one to easily categorize the variety of our experimental data which appears at first puzzling. The main parameter controlling the electron spin polarization is identified to be the ratio of the transit time through these layers to the spin-scattering time in them. The discrepancy between the close to 100% spin injection efficiency we would expect from a half-metal and the 75% we have obtained experimentally might thus originate from spin scattering of electrons in transit to the QW. In other words, our model shows that all of our data are still compatible with Co₂FeSi being a half-metallic injector providing a 100% spin-injection efficiency.

II. EXPERIMENTAL

For the present study, we have used the same type of spin-LEDs as in our previous work which were fabricated in a dual-chamber molecular-beam epitaxy (MBE) system.⁸ The semiconductor structure for all devices investigated here is the same and is virtually identical to the structures used by the group of Palmstrøm⁴ and very similar to those of the groups of Parkin^{5,11,12} and Jonker.^{2,13} Specifically, these devices comprise the following layer sequence grown in the semiconductor-MBE chamber on *p*-type GaAs(001) substrates: 400 nm *p*-GaAs ($p=1 \times 10^{17}$ cm⁻³), 200 nm *p*-Al_{0.1}Ga_{0.9}As ($p=1 \times 10^{16}$ cm⁻³), 50 nm undoped material containing a 10-nm-thick GaAs quantum well sandwiched between 20-nm-thick Al_{0.1}Ga_{0.9}As barriers, 115 nm *n*-Al_{0.1}Ga_{0.9}As (100 nm with $n=1 \times 10^{16}$ cm⁻³ and 15 nm linearly graded from $n=1 \times 10^{16}$ – 5×10^{18} cm⁻³), and 15–25 nm *n*-Al_{0.1}Ga_{0.9}As ($n=5 \times 10^{18}$ cm⁻³). We will focus on three LEDs here: LED #1, which is special since the sample has been exposed to air prior to the Co₂FeSi growth for measuring the polarization response of a bare LED. The Co₂FeSi layer was grown subsequently in the metal MBE chamber at 300 °C. For LED #2, this layer was grown immediately after transfer in ultrahigh vacuum to the metal-MBE growth chamber at 200 °C, and for LED #3, at 300 °C. SIMS measurements have shown that LED #1 con-

tains only comparatively moderate amounts of Co and Fe (10¹⁹ cm⁻³), while LED #2 and #3 contain these elements in abundance (cf. Fig. 1). The majority of the Co and Fe atoms in sample #3 is likely to be not substitutional, but agglomerated.^{8,14,15} LED #3 is exemplary for devices which simply seem to “work,” while LEDs #1 and #2 represent the cases of very low spin-injection efficiency and high spin scattering, respectively.

As in our previous work,⁸ the EL measurements are performed in the Faraday geometry with the LEDs placed in a superconducting magnet system. In the present study, all measurements are done with a magnetic field ranging from –14 to 14 T to enable the detection of both diamagnetic and paramagnetic contributions. Furthermore, the circular polarization degree of the EL is analyzed using gated photon counting with the gate width set to match the frequency of a photoelastic modulator. In comparison to lock-in amplification, which we have used previously, the present technique allows us to detect much weaker EL signals (such as obtained at low forward bias) while retaining a high accuracy in determining the degree of circular polarization $\rho_C=(I_+-I_-)/(I_++I_-)$ [where $I_+(I_-)$ is the intensity of right (left) circularly polarized light].

III. THEORETICAL CONSIDERATIONS

We consider the injection of spin-polarized electrons from the Co₂FeSi layer into the upper (Al,Ga)As layer, their transport through this layer and the accompanying spin relaxation, their capture by the GaAs QW and the spin relaxation therein, and their recombination with holes as described by the following equations:

$$\frac{dn_b^+}{dt} = G^+ - \frac{n_b^+}{\tau_t} - \frac{n_b^+}{\tau_b^+} + \frac{n_b^-}{\tau_b^-} = 0, \quad (1)$$

$$\frac{dn_b^-}{dt} = G^- - \frac{n_b^-}{\tau_t} - \frac{n_b^-}{\tau_b^-} + \frac{n_b^+}{\tau_b^+} = 0, \quad (2)$$

$$\frac{dn_q^+}{dt} = \frac{n_b^+}{\tau_t} - b_r n_q^+ p_q^- - \frac{n_q^+}{\tau_q^+} + \frac{n_q^-}{\tau_q^-} = 0, \quad (3)$$

$$\frac{dn_q^-}{dt} = \frac{n_b^-}{\tau_t} - b_r n_q^- p_q^+ - \frac{n_q^-}{\tau_q^-} + \frac{n_q^+}{\tau_q^+} = 0. \quad (4)$$

Here, $G^\pm = G_0[1 \mp S \tanh(B/B_0)]/2$ represent the injection of spin-up/down electrons (n_b^\pm) into the top (Al,Ga)As layer with an efficiency S . B_0 is chosen in such a way as to fit the experimentally measured magnetization of Co₂FeSi. The transit time through the upper (Al,Ga)As layer is denoted by τ_t and the radiative recombination coefficient in the QW by b_r . The spin-relaxation times for the barrier (b) and the QW (q) must obey $(\tau_i^+ - \tau_i^-)/(\tau_i^+ + \tau_i^-) = \tanh(\Delta E_i/2k_B T_e^i)$ and $1/\tau_i^+ + 1/\tau_i^- = \Gamma_i^s$ with $i=\{b,q\}$ and the electron temperature T_e . The total spin-relaxation rate Γ_i^s has been separately determined for the QW by timed-resolved photoluminescence (PL) (Ref. 8) and is treated as a free parameter for the barrier. The energy splitting ΔE_i reads¹⁶

$$\Delta E_i = g_i \mu_B B + x J N_0 \alpha B_j(z) \quad (5)$$

with $i=\{b, q\}$, the g-factors g_i , and the Bohr magneton μ_B . x denotes the concentration of magnetic ions, J their angular momentum, $N_0 \alpha$ the exchange coupling between the magnetic ions and electrons, and $B_j(z)$ is the Brillouin function with $z = g_M J \mu_B B / k_B T$, where g_M is the g-factor of the magnetic ions.

Spin relaxation of holes (which are injected unpolarized) is assumed to be sufficiently rapid so that spin-up/down holes in the QW attain their thermal equilibrium population given by

$$\frac{p_q^+ - p_q^-}{p_q^+ + p_q^-} = \tanh\left(\frac{\Delta E_v}{2k_B T}\right) \quad (6)$$

with $\Delta E_v = g_v \mu_B B$. The total number of electrons and holes is equal for a perfect Ohmic contact, but for a Schottky contact their relation is given by

$$\frac{n_q^+ + n_q^-}{p_q^+ + p_q^-} = \eta \quad (7)$$

with η depending on the barrier height. Solving the Poisson, drift diffusion, and continuity equations show η to be on the order of 0.1 for a Schottky barrier of, e.g., 0.35 eV height.^{17,18}

Equations (1)–(7) are solved numerically to obtain

$$\rho_c = \frac{n_q^+ p_q^- - n_q^- p_q^+}{n_q^+ p_q^- + n_q^- p_q^+}. \quad (8)$$

Prior to the discussion of experimental results, let us comment on two important parameters introduced above, namely, (i) the spin-scattering time in the (Al,Ga)As layer and (ii) the transit time.

ad (i): The spin-scattering times of electrons is determined by material parameters such as the strength of the spin-orbit coupling. For a given material, doping density and temperature, the spin-scattering time $\tau_s = 1/\Gamma_b^s$ can be safely regarded to be invariant. Since all of our LEDs have an essentially identical design, we would expect an identical spin-scattering time. However, as already reported in Ref. 8 and shown exemplary for two of the present structures in Fig. 1, the top (Al,Ga)As layer contains sizable amounts of both Co and Fe due to in-diffusion of these elements during growth of the Co₂FeSi layer. Because of their magnetic nature, substitutionally incorporated Fe and Co atoms act as a supremely efficient spin-scattering center, thus drastically shortening the spin-scattering time.

ad (ii): The injection of electrons in an LED under forward bias occurs, in general, not ballistically, but under thermalized conditions at small fields. For this simple, classical case, the drift velocity v is well defined as $v = \mu E$ with the mobility μ and the electric field E , and the transit time τ_t is simply given by d/v with the distance d being equal to the thickness of the top (Al,Ga)As layer. The transit time thus strongly depends on the potential profile and the electron mobility in the top (Al,Ga)As layer.¹⁹ In the present case, μ is expected to be sharply reduced and the potential profile strongly altered by the high concentration of incorporated Fe

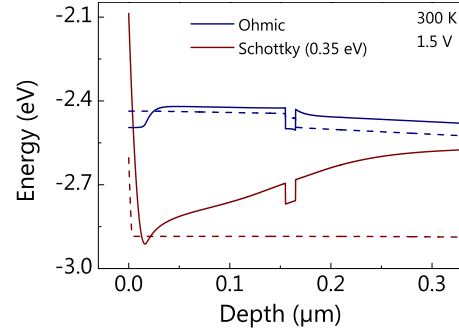


FIG. 2. (Color online) Conduction-band profiles of the top 300 nm of the present LEDs calculated by solving the Poisson, drift diffusion, and continuity equations for a forward bias of 1.5 eV and assuming either an Ohmic or a reversely biased Schottky contact with a barrier height of 0.35 eV. Recombination is assumed to be bimolecular throughout the structure. The dashed lines show the quasi-Fermi levels for electrons.

and Co atoms, which besides their magnetic nature may also act as deep, doubly charged acceptors when incorporated substitutionally. The decreased mobility facilitates the relaxation of injected electrons to the band edge via a vastly increased chance for inelastic scattering. In addition, the Co₂FeSi layer is certainly not a perfect Ohmic, but rather an imperfect and reversely biased Schottky contact. As a consequence, electrons may have to overcome a potential barrier as illustrated by Fig. 2, and the transit time is thus expected to depend on the bias and to vary strongly from sample to sample as it depends on diffusion rather than drift.

Next, let us consider the limiting cases for the ratio between the spin-scattering time and the transit time.

$\tau_s / \tau_t \gg 1$: in this case, spin scattering in the top (Al,Ga)As layer can be neglected, and the nonequilibrium spin polarization due to spin injection is thus fully preserved during the transit to the QW.

$\tau_s / \tau_t \ll 1$: under this condition, the spin polarization of the electrons will reach thermal equilibrium according to the Zeeman splitting in the top (Al,Ga)As layer, inhibiting the observation of spin injection. As a consequence, the polarization of the EL reflects the spin splitting in the conduction band, which is characteristic for the respective material and is described by the Brillouin function term in Eq. (5) for the case of a paramagnetic DMS.

IV. RESULTS AND DISCUSSION

We first analyze the polarization response of a bare LED structure (LED #1) *before* deposition of a spin-injection layer (i. e., $G^+ = G^- = 0.5$ and $x = 0$), but instead with an Ohmic contact (i. e., $\eta = 1$) for electron injection. The dependence of the polarization degree on magnetic field for this reference LED is displayed in Fig. 3(a). The shape of this polarization response is solely determined by the g-factors g_b , g_q , and g_v . The fit of Eq. (8) yields $g_b = -0.1$, $g_q = -0.2$, and $g_v = 0.065(1 + |B/B_1|)$ with $B_1 = 1$ T. These values are similar to g-factors reported in the literature.^{20,21} The latter two of these values will be kept fixed in all that follows. For the

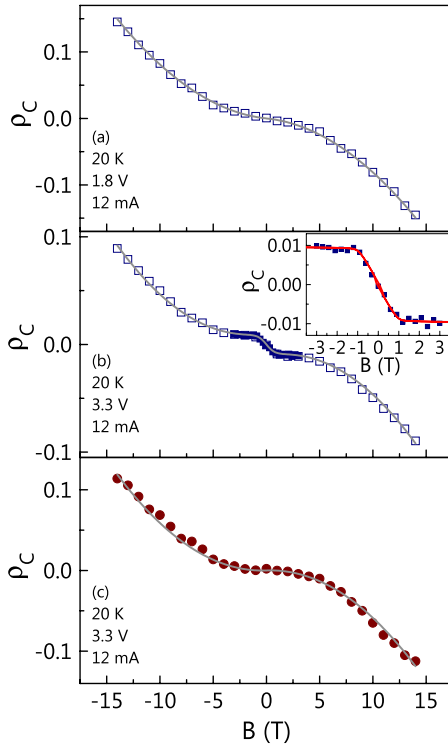


FIG. 3. (Color online) Degree of circular polarization ρ_C of the EL at 20 K from LED #1. The symbols indicate experimental data, while the solid lines represent the result of a simulation according to Eq. (8). Plot (a) shows the device prior to deposition of a Co_2FeSi injection layer, (b) after, and (c) after etching this layer off. The inset in (b) shows a comparison of ρ_C with the actual magnetization of Co_2FeSi at 5 K (solid line).

comparison of LEDs before and after removal of the Co_2FeSi injection layer, the experimental data are fit with the same parameters, but using $|S|=0$ for the LED after removal of the Co_2FeSi layer. In this way, we have been able to reproduce all experimental results in a consistent manner using reasonable parameters.

Figure 3(b) shows the polarization response of the same LED with a subsequently deposited Co_2FeSi injection layer. Evidently, the overall shape of the curve is similar, although a much higher bias is required for attaining the same current level (the higher bias is due to the reversely biased Schottky characteristics of the electric contact provided by the Co_2FeSi injection layer as visualized by Fig. 2). Most important, however, is the ferromagnetic signature at small magnetic fields, as highlighted in the inset. The polarization response (symbols) and magnetization of this Co_2FeSi layer at 5 K (solid curve) match exactly, demonstrating that the small-field behavior is indeed due to spin injection from the ferromagnetic injector.

Evidently, the polarization of about 1% measured at the saturation field of about 1.5 T is comparatively small. Two mechanisms may be responsible for this result: first, the spin-injection efficiency itself may be low and second, spin flip may occur during transport of electrons to the QW. We stress that, strictly speaking, our model cannot be used for distinguishing these two different scenarios, as it can fit the experiment equally well for either mechanism. However, it is

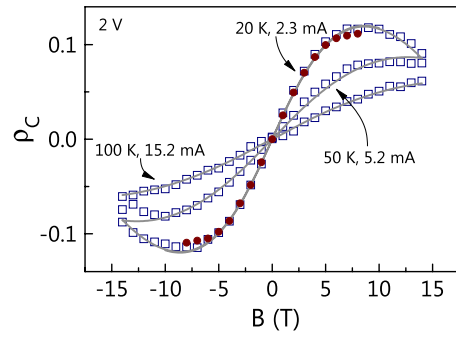


FIG. 4. (Color online) Degree of circular polarization ρ_C of the EL at different temperatures from LED #2. The open symbols indicate experimental data, while the solid lines represent the results of simulations according to Eq. (8). The solid symbols denote the results obtained after etching the Co_2FeSi layer off.

evident that the shape observed in Figs. 3(a) and 3(b) is basically identical at large magnetic fields, reflecting a negligible spin scattering during transport to the QW. In fact, SIMS depth profiles for this sample (not shown here) reveal a comparatively low (10^{19} cm^{-3}) concentration of Co and Fe. Moreover, this particular sample has been exposed to air prior to the growth of the Co_2FeSi layer to obtain the data displayed in Fig. 3(a). Although we have taken precautions for regrowth, we cannot exclude a residual oxide at the interface that promotes spin flip. We thus believe that this sample is a likely candidate for an inherently low spin-injection efficiency and a long spin-relaxation time ($\tau_s/\tau_t=2.0$ for $|S|=0.03$). Figure 3(c) shows the polarization of LED #1 after the Co_2FeSi layer has been etched off, and an electric (Schottky) contact has been made by Ti. The electric characteristics is thus virtually identical to that shown in Fig. 1(b), but the ferromagnetic component has disappeared entirely, confirming the interpretation above. Note that we have only changed the value of η and x for the simulations displayed in Figs. 3(a)–3(c).

Figure 4 shows the polarization response of LED #2 for three different temperatures. Obviously, the behavior observed is a purely paramagnetic one, suggesting a complete realignment of the spin-polarized electrons injected from the Co_2FeSi layer. This realignment is a result of an ultrashort spin-relaxation time ($\tau_s/\tau_t=0.002$ for $|S|=1.0$). In fact, we obtain exactly the same result after the removal of the Co_2FeSi layer (solid symbols), demonstrating the transformation of the top (Al,Ga)As layer into a paramagnetic DMS by Co and Fe in diffusion. In other words, the memory of spin injection is erased entirely by spin realignment in the paramagnetic DMS. The value assumed for $|S|$ is thus arbitrary and may lie between 0 and 1. The signature of spin alignment in such DMS-type layers can be immediately recognized by the positive slope in the magnetic field dependence of ρ_C for $|B| < 8$ T. The negative slope at larger B fields reflects the contribution of the spin alignment in the QW, resembling the behavior of the bare LED #1. The fits of the experimental results as shown in Fig. 4 are performed with a lattice temperature T as indicated in the figure, but with an electron temperature T_e of 50 (100 for $T=100$ K) and 100 K for the QW and the barrier, respectively. Consid-

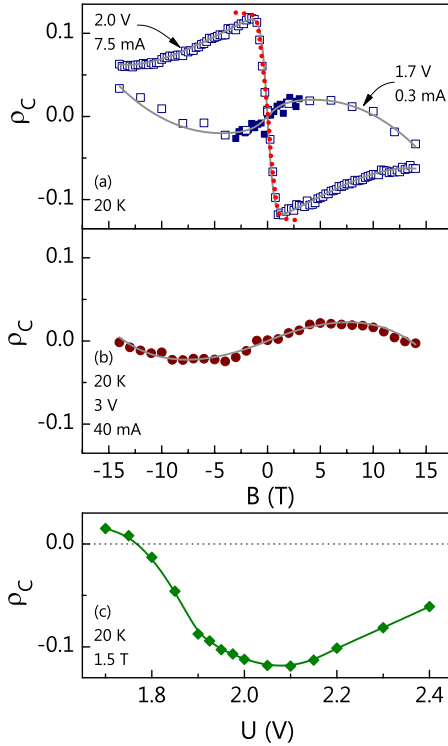


FIG. 5. (Color online) Degree of circular polarization ρ_C of the EL at 20 K from LED #3. The symbols indicate experimental data, while the solid lines represent the results of simulations according to Eq. (8). Plot (a) shows the EL polarization at two different voltages. For the measurements taken at 1.7 V, two sets of experiments are shown (open and solid squares). The dotted line displays the magnetization of this sample. Plot (b) shows the results after etching the Co_2FeSi layer off. Plot (c) summarizes the peak polarization of this sample as a function of the bias. The solid line is a guide to the eyes and the dashed line denotes zero.

ering the comparatively high voltage applied and the rather high resulting currents, these values do not appear unreasonably high. Note that the complete absence of any ferromagnetic signature in Fig. 4 demonstrates that artifacts resulting from magneto-optic effects due to the transmission of the EL through the ferromagnetic injector are entirely negligible in our experiments.

Figure 5 shows the same measurement for LED #3, for which the Co_2FeSi layer has been deposited *in situ* at 300 °C. Figure 5(a) displays the data for two different voltages. At low voltage (1.7 V), the behavior observed reflects the situation of strong spin scattering and thus exhibits qualitatively the same characteristics as LED #2. For just slightly higher voltages (>1.9 V), the polarization response is reversed and at low fields dominated by a ferromagnetic signal as evidenced by the agreement with the magnetization of this Co_2FeSi layer at 5 K (dotted line). For this particular sample and bias, the polarization degree has an absolute value of about 12%, corresponding to a minimum spin-injection effi-

ciency of 36% considering the exciton and spin lifetimes deduced from time-resolved PL measurements. Tuning the bias voltage hence allows us to reach a regime of medium-strength spin scattering ($\tau_s/\tau_t=0.42$ for $|S|=1.0$) for which spin injection prevails. The fit of the experimental data is compatible with a spin-injection efficiency between $0.36 \leq |S| \leq 1$. Figure 5(b) shows the response obtained from the same sample after the Co_2FeSi layer has been etched off. Evidently, the results obtained are very similar to those presented in Fig. 5(a) at 1.7 V. In particular, the small-signal response is still paramagnetic, evidencing an irreversible change in the top (Al,Ga)As layer upon growth of the Co_2FeSi layer. Furthermore, we can exclude any contribution of the (Fe,Co) agglomerates in the top (Al,Ga)As layer to the ferromagnetic signature in Fig. 5(a).

In Fig. 5(c), we show the dependence of the peak EL polarization (at a fixed magnetic field of 1.5 T) on bias for sample #3. We observe a paramagnetic behavior up to 1.8 V, but an abrupt change to a ferromagnetic one for higher voltages, as it is evident from the sign reversal in the EL polarization. The maximum polarization of 14% is reached at 2.1 V (the reduction observed for even higher voltages is caused by heating, which manifests itself in a redshift of the emission wavelength). The bias voltage influences essentially the transit time, whereas the impact on the spin-scattering rate can be neglected.¹⁹ Within our model, the abrupt transition from a paramagnetic behavior (induced by spin alignment) to a ferromagnetic one due to spin injection is determined by the ratio of the transit time through the barrier (τ_t) and the spin-relaxation time (τ_s).

V. CONCLUSION

In conclusion, taking into account spin alignment in the topmost layer of our spin LEDs, the rate-equation model presented above reproduces our experimental results in a consistent manner using physically reasonable parameters. Due to the very high concentration (up to, effectively, 1%) of magnetic impurities in this layer, spin scattering may be up to three orders of magnitude faster than the transit time. Since diffusion of Co and Fe is most likely not only a problem for the growth of Co_2FeSi but also for other (Co,Fe) compounds grown on *n*-type (Al,Ga)As, spin scattering in the topmost layer of spin LEDs cannot be neglected *a priori* when evaluating the spin-injection efficiency.

ACKNOWLEDGMENTS

We thank Walid Anders for the processing of the spin LEDs, Gerd Paris for the design and construction of a controller for gated photon counting, and Pawel Bruski and Rouin Farchi for their measurements on very recent spin LEDs and many other valuable contributions. Finally, we are indebted to Steven C. Erwin (Naval Research Laboratory) for critically reading the manuscript and *ab initio* calculations regarding Co_2FeSi in both the B2 and L2₁ structure.

*brandt@pdi-berlin.de

- ¹H. J. Zhu, M. Ramsteiner, H. Kostial, M. Wassermeier, H.-P. Schönherr, and K. H. Ploog, *Phys. Rev. Lett.* **87**, 016601 (2001).
- ²A. T. Hanbicki, B. T. Jonker, G. Itskos, G. Kioseoglou, and A. Petrou, *Appl. Phys. Lett.* **80**, 1240 (2002).
- ³V. F. Motsnyi, P. Van Dorpe, W. Van Roy, E. Goovaerts, V. I. Safarov, G. Borghs, and J. De Boeck, *Phys. Rev. B* **68**, 245319 (2003).
- ⁴C. Adelman, X. Lou, J. Strand, C. J. Palmstrøm, and P. A. Crowell, *Phys. Rev. B* **71**, 121301(R) (2005).
- ⁵X. Jiang, R. Wang, R. M. Shelby, R. M. Macfarlane, S. R. Bank, J. S. Harris, and S. S. P. Parkin, *Phys. Rev. Lett.* **94**, 056601 (2005).
- ⁶M. Ramsteiner, H. Y. Hao, A. Kawaharazuka, H. J. Zhu, M. Kästner, R. Hey, L. Däweritz, H. T. Grahn, and K. H. Ploog, *Phys. Rev. B* **66**, 081304(R) (2002).
- ⁷B. Liu, M. Sénès, S. Couderc, J. F. Bobo, X. Marie, T. Amand, C. Fontaine, and A. Arnoult, *Physica E (Amsterdam)* **17**, 358 (2003).
- ⁸M. Ramsteiner, O. Brandt, T. Flissikowski, H. T. Grahn, M. Hashimoto, J. Herfort, and H. Kostial, *Phys. Rev. B* **78**, 121303(R) (2008).
- ⁹M. Hashimoto, J. Herfort, H.-P. Schönherr, and K. H. Ploog, *J. Appl. Phys.* **98**, 104902 (2005).
- ¹⁰M. Hashimoto, J. Herfort, A. Trampert, H.-P. Schönherr, and K. H. Ploog, *J. Vac. Sci. Technol. B* **24**, 2004 (2006).
- ¹¹G. Salis, R. Wang, X. Jiang, R. M. Shelby, S. S. P. Parkin, S. R. Bank, and J. S. Harris, *Appl. Phys. Lett.* **87**, 262503 (2005).
- ¹²R. Wang, X. Jiang, R. M. Shelby, R. M. Macfarlane, S. S. P. Parkin, S. R. Bank, and J. S. Harris, *Appl. Phys. Lett.* **86**, 052901 (2005).
- ¹³A. T. Hanbicki, O. M. J. van't Erve, R. Magno, G. Kioseoglou, C. H. Li, and B. T. Jonker, *Appl. Phys. Lett.* **82**, 4092 (2003).
- ¹⁴S. Hirose, M. Yamaura, S. Haneda, K. Hara, and H. Munekata, *Thin Solid Films* **371**, 272 (2000).
- ¹⁵R. Moriya, Y. Katsumata, Y. Takatani, S. Haneda, T. Kondo, and H. Munekata, *Physica E (Amsterdam)* **10**, 224 (2001).
- ¹⁶W. Heimbrod *et al.*, *Physica E (Amsterdam)* **10**, 175 (2001).
- ¹⁷D. W. Winston, SIMWINDOWS 1.50, <http://scripts.mit.edu/sunxc/research/tools/simwin.html>
- ¹⁸D. W. Winston, Ph.D. thesis, University of Colorado at Boulder, 1996.
- ¹⁹P. Van Dorpe, W. Van Roy, V. F. Motsny, G. Borghs, and J. De Boeck, *J. Vac. Sci. Technol. A* **22**, 1862 (2004).
- ²⁰M. J. Snelling, G. P. Flinn, A. S. Plaut, R. T. Harley, A. C. Tropper, R. Eccleston, and C. C. Phillips, *Phys. Rev. B* **44**, 11345 (1991).
- ²¹M. J. Snelling, E. Blackwood, C. J. McDonagh, R. T. Harley, and C. T. B. Foxon, *Phys. Rev. B* **45**, 3922 (1992).